Des-A-lupane in an East African lake sedimentary record as a new proxy for C_3-plant stable carbon isotopic composition

L.G.J. van Bree[a,b*], W.I.C. Rijpstra[a], N.A. Al-Dhabi[c], D. Verschuren[d], J.S. Sinninghe Damsté[a,b], J.W. de Leeuw[a,b]

[a] NIOZ Royal Netherlands Institute for Sea Research, Department of Marine Microbiology and Biogeochemistry, and Utrecht University, PO Box 59, 1790 AB Den Burg, The Netherlands.

[b] Utrecht University, Faculty of Geosciences, Department of Earth Sciences, PO Box 80.115, 3508 TC Utrecht, The Netherlands.

[c] Department of Botany and Microbiology, Addiriyah Chair for Environmental Studies, College of Science, King Saud University, P.O. Box 2455, Riyadh 11451, Saudi Arabia.

[d] Ghent University, Limnology Unit, K.L. Ledeganckstraat 35, B-9000 Gent, Belgium.

*Corresponding author. Utrecht University, Faculty of Geosciences, Department of Earth Sciences, PO Box 80.115, 3508 TC Utrecht, The Netherlands. L.G.J.vanBree@uu.nl. +31 30 253 52 32

To be submitted to *Organic Geochemistry*

Abstract

We studied the high-resolution and well-dated 25,000 year sedimentary record of Lake Challa, a deep tropical crater lake in equatorial East Africa, to explore new proxies for paleoenvironmental and paleohydrological change. Sedimentary biomarker analysis revealed the presence of *des*-A-triterpenoids with oleanane, ursane and lupane carbon skeletons, microbial degradation products of angiosperm plant triterpenoids. Their increased influx from 16,000 years ago corresponds with previously documented changes in the terrestrial vegetation of the Lake Challa basin during postglacial warming, in particular the relative increase in C_3/C_4 plant ratio inferred from the stable carbon isotopic signature ($\delta^{13}C$) of sedimentary *n*-alkanes derived from plant leaf waxes. In contrast to this *n*-alkane $\delta^{13}C$, the $\delta^{13}C$ of *des*-A-lupane maintains a constant value of -27.4±1.1‰ across the glacial–interglacial transition. Since *des*-A-lupane is derived from C_3 plants, its $\delta^{13}C$ signature is here proposed to represent a novel and independent proxy for the time-variable carbon isotopic composition of local terrestrial C_3 plants, which can improve estimates of the C_3/C_4 plant ratio based on two-end member mixing models of *n*-alkane $\delta^{13}C$ values.

Keywords

Des-A-triterpenoids; *des*-A-lupane; $\delta^{13}C$ of *des*-A-lupane; lacustrine sediments; East Africa; C_3/C_4 plant ratio; vegetation reconstruction.

1. Introduction

Non-hopanoid pentacyclic triterpenoids preserved in lake and marine sediments are relatively well studied biomarkers, and used in organic geochemistry as a proxy for the input of terrestrial angiosperm plants (e.g. Rullkötter et al., 1982; Freeman et al., 1994; Sabel et al., 2005). These wax components are synthesized almost exclusively by higher plants as a defense mechanism against insects, pathogens and herbivores (Langenheim, 1994). Pentacylic triterpenoids with, for example, lupane, oleanane and ursane skeletons, are widely accepted as general biomarkers for angiosperms, yet most of these triterpenoids are not species-specific (e.g. Ohmoto et al., 1970; ten Haven and Rullkötter, 1988; Regnery et al., 2013). *Des*-A-triterpenoids, in turn, are diagenetic products of triterpenoid A-ring degradation (Trendel et al., 1989), a process probably mediated by microorganisms under anoxic conditions (Lohmann et al., 1990).

Plant wax lipids, such as *n*-alkanes, can be used as indicators of the composition of local vegetation, as their compound-specific stable carbon isotopic value ($\delta^{13}C$) depends on the dominant biochemical pathway used by plants for photosynthesis. Higher plants usually fix CO_2 by either the C_3 (Calvin-Benson) or C_4 (Hatch-Slack) cycle. In C_4 photosynthesis, atmospheric CO_2 entering the plant stomata is pre-concentrated, resulting in less carbon isotopic depletion. In tropical Africa, lowland vegetation consists mostly of C_4 grasses and C_3 trees and shrubs, and (seasonal) moisture availability is the dominant control on the distribution and abundance of these C_4 grasses across the modern-day landscape. On glacial-interglacial time scales, variation in atmospheric pCO_2 exerted important control on the composition of savanna vegetation of East Africa (Sinninghe Damsté et al., 2011). When pCO_2 varies little, as within the Holocene, the distribution of C_3 and C_4 vegetation can be used as a measure of past water availability (Castañeda et al., 2007).

66 During an earlier high-resolution stratigraphic study of *n*-alk-1-enes in the continuous
67 and well-dated 25,000-year (25 kyr) sedimentary record of Lake Challa, a deep crater lake in
68 equatorial East Africa (van Bree et al., 2014), we also encountered a wide range of *des*-A-
69 triterpenoids. In this paper, we report our findings regarding the origin and potential
70 paleoenvironmental application of the pentacyclic triterpenoid degradation products derived
71 from higher plants. A study of *des*-A-arborenes/fernenes also present in Lake Challa
72 sediments, but of microbial origin, will be published separately.
73
74 **2. Material and Methods**
75 2.1 Study area
76 Lake Challa (3°19'S, 37°42'E) is a relatively unproductive, tropical freshwater lake, situated
77 ~880 m above sea level on the lower south-eastern slope of Mt. Kilimanjaro (Fig. 1). Shared
78 by Kenya and Tanzania, it has a surface area of 4.5 km^2, a steep-sided crater catchment of
79 ~3.4 km^2 and a maximum depth of ~90 m. Rainfall seasonality is mainly determined by the
80 semi-annual passing of the Inter-Tropical Convergence Zone (ITCZ), resulting in moderate
81 'long rains' (March-May) and more intense 'short rains' (October-December) separated by a
82 long dry season during Southern Hemisphere winter (June-September). Since the local
83 balance between precipitation and evaporation is negative by three to one, the lake's water
84 budget must be maintained by substantial groundwater inflow, derived from rainfall on the
85 forested mid-elevation slopes of Mt. Kilimanjaro. Also temporary creek discharge breaching
86 the crater's northwestern rim can occur during very heavy rains (Buckles et al., 2014). Daily
87 wind-driven mixing of the water column is limited to the uppermost 15-20 m year-round.
88 Seasonal deeper mixing (June-September) extends to 40-60 m, implying a permanently
89 stratified lower water column. Given limited density stratification, the possibility of complete
90 mixing cannot be excluded but its recurrence frequency is likely decadal or longer, rather than

inter-annual (Wolff et al., 2011, 2014). Wind-blown (aeolian) particles, supplemented by soil and litter input from the steep-sided inner slopes of the crater, contribute allochthonous organic matter to Lake Challa sediments. The vegetation outside the crater and on top of the rim is a woodland-savannah with shrubs, trees and C_4 grasses, while inside the crater rim a more varied vegetation occurs, including CAM plants in a dry succulent forest occupying the middle slopes, and a fringe of evergreen forest around the lake shore (Hemp, 2006; Sinninghe Damsté et al., 2011).

2.2 Study material

A 21.65 m composite core of mostly finely-laminated organic muds was retrieved from the center of Lake Challa (Fig. 1) during coring activities in 2003 and 2005 (Verschuren et al.,2009). This yielded, after excision of five turbidites, a 20.82 m long master sequence covering the last 25 kyr of continuous offshore lacustrine sedimentation. The age-depth model is based on a smoothed spline through INTCAL04-calibrated AMS ^{14}C ages of 164 bulk organic carbon samples (Blaauw et al., 2011). For this study, a total of 148 sediment samples with 4-cm thickness were extracted and processed for biomarker analysis, generally at ~200-year intervals, with a higher resolution of ~50 year intervals in the youngest 3.2 kyr. In addition, we analyzed the compound-specific $\delta^{13}C$ of selected biomarkers in 52 sediment samples distributed throughout the sequence.

In order to trace the origin of the biomarkers found in Lake Challa sediments, we further analyzed soil and litter samples from around the lake, suspended particulate matter (SPM) and settling particles collected by a sediment trap (Sinninghe Damsté et al. 2009; Buckles et al. 2014). This sediment trap was deployed at 35 m water depth in a most often suboxic part of the water column, and samples were retrieved at ca. 4-week intervals between November 2006 and December 2007 (Sinninghe Damsté et al., 2009). The SPM sampling was

conducted on 10–11 September 2006 along a vertical profile in the center of the lake, every 5 m between 0 and 30 m, and every 10 m between 30 and 90 m water depth. The water samples (4 to 9 L) were filtered through GF/F filters and stored frozen until processing. Eight soil samples were collected from within the catchment area of Lake Challa in 2005 (Sinninghe Damsté et al., 2009; Fig. 1). Sampling of litter in September 2012 included three near-shore samples representing leaf and fruit remains from forest trees and shrubs, and two samples from just below the crater rim consisting of leaf and twig remains and small non-diagnostic organic debris. These samples were also stored frozen until analysis.

2.3 Lipid extraction

The freeze-dried and powdered sediment samples were extracted with a Dionex™ Accelerated Solvent Extractor (ASE), using a dichloromethane (DCM)/methanol (9:1, v/v) mixture at high temperature (100°C) and pressure (7.6 x 106 Pa) (Sinninghe Damsté et al., 2011). The total extracts were separated over an activated Al_2O_3 column into an apolar and a polar fraction with hexane/DCM (9:1, v/v) and DCM/MeOH (1:1, v/v), respectively. Accumulation rates of apolar compounds (in mg m^{-2} yr^{-1}) were calculated based on their concentration, the wet weight and water content of the sediment samples, and the sediment's age-depth profile. For analysis of stable carbon isotopic composition, a subset of the apolar fractions were separated into a saturated and an unsaturated hydrocarbon fraction using a small Ag^+-impregnated silica column with hexane and ethyl acetate as eluents, respectively.

SPM and sediment trap samples were extracted previously (Sinninghe Damsté et al., 2009). Fluxes of apolar compounds (in mg m^{-2} yr^{-1}) in the sediment trap samples were calculated using the concentration of each of these components relative to total particle flux.

Litter and soil samples were extracted ultrasonically with DCM/MeOH (2:1, v/v), after cutting the larger leaf, stem or fruit remains into small pieces. The extracts were evaporated to

dryness, methylated with diazomethane in diethyl ether and separated over an activated Al_2O_3 column into apolar, ketone and polar fractions, using hexane/DCM (9:1, v/v), hexane/DCM (1:1, v/v) and DCM/MeOH (1:1, v/v) as eluents, respectively.

2.4 Lipid identification and quantification

The apolar fractions of sediments, SPM, sediment trap, soil and litter extracts were analyzed by gas chromatography (GC) and GC-mass spectrometry (GC/MS), after addition of a known amount of internal standard. A few polar fractions of sediment and SPM samples were methylated, silylated and screened for functionalized triterpenoids.

GC was performed using a Hewlett-Packard (HP6890) instrument equipped with an on-column injector and a flame ionization detector (FID). A fused silica capillary column (25 m x 0.32 mm) coated with CP Sil-5 CB (film thickness 0.12 µm) was used with helium as carrier gas. The samples were injected at 70°C and the oven temperature was programmed to rise at 20°C/min to 130°C, and then at 4°C/min to 320°C, at which it was held for 20 min.

GC-MS was performed on a Finnigan Trace DSQ mass spectrometer operated at 70 eV with a mass range of *m/z* 40 to 800 and a cycle time of 1.7 s. The gas chromatograph was equipped with a fused silica capillary column as described above. The carrier gas was helium and the same oven temperature program as for GC was used. Identification of the *des*-A-triterpenoids and other triterpenoid hydrocarbons is based on relative retention times, published mass spectra (including the NIST98 spectral library), and interpretation of observed fragmentation patterns. Quantification of compounds was performed by peak area integration of appropriate peaks (including that of the internal standard) in the FID chromatograms.

2.5 Compound-specific carbon isotope analyses

We subjected 52 saturated hydrocarbon fractions to compound-specific $\delta^{13}C$ analysis using an Agilent 6800 GC coupled to a ThermoFisher Delta V isotope-ratio monitoring mass spectrometer. The isotope values were measured with reference to a calibrated external reference gas, and performance of the instrument was monitored daily by injections of a mixture of a C_{20} and a C_{24} perdeuterated *n*-alkane with known isotopic composition. The $\delta^{13}C$ values are reported in standard delta notation against the Vienna Pee Dee Belemnite (VPDB). All samples were run at least in duplicate, allowing estimation of the standard deviation of these measurements. $\delta^{13}C$ values of the *n*-alkanes in these same samples have been published previously (Sinninghe Damsté et al., 2011).

3. Results

3.1 The sedimentary record of *des*-A-triterpenoids in Lake Challa

Our analysis of the apolar fractions of 148 biomarker extracts from Lake Challa sediments covering the last 25 kyr showed the presence of *n*-alkanes, *n*-alk-1-enes, phytadienes, aromatic triterpenoids, hopenes, and a suite of *des*-A-triterpenoid hydrocarbons with lupane, oleanane, ursane, and fernane or arborane skeletons. The stratigraphic distribution, origin and palaeoenvironmental significance of the *n*-alkanes and *n*-alk-1-enes have been discussed by Sinninghe Damsté et al. (2011) and van Bree et al. (2014), respectively.

We detected 11 distinct *des*-A-triterpenoid hydrocarbon compounds on the basis of on their relative retention times, published mass spectra, and interpretation of mass spectrometric fragmentation patterns. The mass spectra of ten *des*-A-triterpenes and one *des*-A-triterpane exhibit molecular ions at *m/z* 324, 326, 328 or 330. In this paper we focus on the distribution, origin and potential paleoenvironmental application of the five *des*-A-triterpenoids with lupane, oleanane and ursane skeletons (Fig. 2A). The identification and geochemical significance of the other, arborane- or fernane-derived *des*-A-triterpenoids will be discussed

elsewhere. Next to these *des*-A-triterpenoids with arborane or fernane skeleton, several other, non-identified *des*-A-triterpenoids co-elute, occur infrequently or in low relative abundance and are not further discussed.

Compound **1** ($M^{+\bullet}$ at *m/z* 328; Fig. 2B) was identified as *des*-A-olean-13(18)-ene (Corbet, 1980; Logan and Eglinton, 1994; Jacob et al., 2007; Huang et al., 2008), and compound **2** ($M^{+\bullet}$ at *m/z* 328; Fig. 2B) was tentatively assigned to *des*-A-olean-12-ene (Corbet, 1980; Logan and Eglinton, 1994; Jacob et al., 2007). *Des*-A-triterpenoid **3** ($M^{+\bullet}$ at *m/z* 328; Fig. 2B) was identified as *des*-A-urs-13(18)-ene (Corbet, 1980; Logan and Eglinton, 1994; Jacob et al., 2007). Compound **4** ($M^{+\bullet}$ at *m/z* 328; Fig. 2B) represents a mixture of *des*-A-ursenes, which could not be further identified. *Des*-A-triterpenoid **5** exhibiting an $M^{+\bullet}$ at *m/z* 330 (Fig. 2B) was identified as *des*-A-lupane (Corbet, 1980; Schmitter et al., 1981; Trendel et al., 1989; Boreham et al., 1994; Jacob et al., 2007; Huang et al., 2008).

The accumulation rates (in mg m^{-2} yr^{-1}) of these *des*-A-triterpenoid hydrocarbons in the sedimentary record vary considerably over time (Fig. 3). The stratigraphic distributions of *des*-A-triterpenoids with lupane (**5**), ursane (**3**) and oleanane (**1**+**2**) skeletons are all similar and significantly inter-correlated: *des*-A-lupane with *des*-A-oleanenes (R^2=0.53), *des*-A-oleanenes with *des*-A-ursene (R^2=0.62) and *des*-A-lupane with *des*-A-ursene (R^2=0.81). Throughout the record, *des*-A-lupane is more abundant than *des*-A-ursene, whereas *des*-A-oleanenes concentration is lowest (Fig. 3). They all exhibit low accumulation rates from 25,000 to 15,000 years ago (the glacial and early post-glacial period) and much higher (on average 5 to 11 times) accumulation rates in last 12,000 years (the Holocene).

The $\delta^{13}C$ values of *des*-A-lupane (Fig. 4) vary between -25.1‰ and -29.4‰ (-27.4‰±1.1‰ on average) with no significant trend over time (R^2=0.042; *n*=38; p=0.22). Determinations of $\delta^{13}C$ of other *des*-A-triterpenoids of the oleanane and ursane type in the unsaturated hydrocarbon fraction were unsuccessful due to co-elution or low abundances.

3.2 Triterpenoids and *des*-A-triterpenoids in soil and litter surrounding the lake

No *des*-A-triterpenoids were identified in the hydrocarbon fraction of extracts from soils and litter. Functionalized triterpenoids in soils along the crater rim (Fig. 1) were identified as urs-12-en-3β-ol (α-amyrin), olean-12-en-3β-ol (β-amyrin), olean-13(18)-en-3β-ol, ursa-9(11),12-dien-3-one, taraxerone, lup-20(29)-en-3-one, lup-20(29)-en-3-ol acetate and friedelan-3-one and, tentatively, methyl-ursa-2,12-dien-28-oate. Also three pentacyclic triterpene methyl ethers (PTMEs) with oleanane and taraxerane skeletons were detected: 3β-methoxy-olean-12-ene (iso-sawamilletin; β-amyrin ME), 3β-methoxy-olean-18-ene ME (miliacin; germanicol ME) and 3β-methoxy-taraxer-14-ene (sawamilletin, crusgallin or taraxerol ME). Litter samples contained the oleanane-type triterpenoids β-amyrenone, olean-18-en-3β-one (germanicone), olean-18-en-3β-ol (germanicol) and β-amyrin acetate. The functionalized ursane-type triterpenoids present were α-amyrinone and α-amyrin acetate. One litter sample contained a lupeol acetate.

3.3 *Des*-A-triterpenoids in sedimenting particles and suspended particulate matter

In the extracts of sedimenting particles, only low concentrations of *des*-A-urs-13(18)-ene and *des*-A-lupane were detected, next to traces of functionalized triterpenoids such as α-amyrin. Hydrocarbon concentrations in the SPM extracts were too low for identification of specific triterpenoid compounds.

4. Discussion

The strong correlation between accumulation rates of *des*-A-oleanenes, *des*-A-ursene and *des*-A-lupane (Fig. 3) suggest a common origin for these *des*-A-triterpenoids. Higher plant material originates predominantly from washed-in debris of local terrestrial vegetation from

within the crater catchment, because of the absence of riverine input, the limited amount of leaf waxes deposited from the air, and the near-absence of submerged or emergent aquatic macrophytes due to the steep crater walls both above and below the lake surface (Sinninghe Damsté et al., 2011). While various *des*-A-triterpenoid hydrocarbons are present both in the sediment record and to some extent in settling particles, these compounds are lacking in the collected litter and soil. *Des*-A-triterpenoids are thought to result from microbial degradation of functionalized triterpenoids, under anoxic or reducing conditions (e.g. Lohmann et al., 1990; Jacob et al., 2007; Huang et al., 2008);their presence in the sediment trap material indicates that microbial degradation is not restricted to the anoxic lower water column in Lake Challa. One other mechanism for *des*-A-triterpenoids to enter the system, namely the washing-in of microbial degradation products from (anoxic) soils, is unlikely in Lake Challa, as the studied litter and soils did not contain *des*-A-triterpenoids.

The principal degradation processes affecting pentacyclic triterpenoids have been described by various authors (e.g. Trendel et al., 1989; Hauke et al., 1992a, 1992b; Jacob et al., 2007), although not all transformation routes are completely established. Early diagenetic degradation of C-3 oxygenated triterpenoids involves either A to D-ring aromatization or the loss of the A-ring, followed by progressive aromatization from ring B to D (Trendel et al., 1989; Lohmann et al., 1990). The dominant transformation pathway of non-hopanoid triterpenoids in Lake Challa sediments is loss of the A-ring. This loss can be initiated by the formation of A-seco-intermediates, a process that can already occur within the vegetation by photochemical or photomimetic influences (Corbet, 1980; Baas, 1985), but in Lake Challa sediments such intermediates were not identified.

4.1 *Des*-A-oleanenes and *des*-A-ursenes

Oleanane- and ursane-type triterpenoids are generally considered to be biomarkers of terrestrial higher plants, specifically angiosperms (e.g. Diefendorf et al., 2012). Smetanina et al. (2001) identified miliacin (3β-methoxy-olean-18-ene) in a marine fungus, which would imply that oleanoid-type triterpenoids are not exclusively produced by terrestrial higher plants. However, a new study on this fungal species did not yield any miliacin (Bossard et al., 2013). We therefore consider all oleanane- and ursane-type triterpenoids as angiosperms biomarkers.

Functionalized triterpenoids with ursane and oleanane skeletons occur in the local vegetation, soils and litter of Lake Challa, often as α- or β-amyrin. The accumulation of their *des*-A-counterparts in the sediments increased markedly from 15 kyr BP onwards (Fig. 3). A comparatively low accumulation of higher plant *des*-A-triterpenes occurred during the C_4-plant dominated glacial and early late-glacial periods (Sinninghe Damsté et al., 2011; Fig. 4), suggesting that the C_4 grasses which dominated the vegetation inside the crater at that time did not produce (much of these) triterpenoids. The increase in higher plant *des*-A-triterpenoid accumulation after 15 kyr BP (Fig. 3) broadly coincides with the shift towards a mixed C_3/C_4 vegetation as inferred from $\delta^{13}C$ signature of *n*-C_{31} alkanes (Fig. 4; Sinninghe Damsté et al., 2011) and palynological data (van Geel et al., 2011), following the post-glacial intensification of the region's monsoon rainfall (Verschuren et al., 2009).

Concentrations of *des*-A-oleanenes in Lake Challa sediments are relatively low compared to the other *des*-A-triterpenoids, especially considering the predominance of oleanane-type functionalized triterpenoids in the investigated soils and litter. Future studies on the hydrocarbons in local Lake Challa vegetation might shed light on this apparent discrepancy. Possibly, aromatization of some triterpenoid types is favored over the loss of the A-ring, although the low and infrequent occurrence of aromatic triterpenoids in the sedimentary record does not seem to fit this scenario.

289

290 4.2 *Des*-A-lupane: a tracer of C_3-plant vegetation composition

291 The only saturated *des*-A-triterpenoid present in Lake Challa sediments is *des*-A-lupane, as
292 has also been reported from other late-Quaternary lake-sediment records (see e.g. Jacob et al.,
293 2007; Huang et al., 2008). This saturation may be a result of its specific precursors such as
294 lupeol, lupanol or lupanone, or because *des*-A-lupane is more resistant to diagenesis
295 compared to other saturated *des*-A-triterpenoids (Jacob et al., 2007; Huang et al., 2008).

296 *Des*-A-lupane records have been interpreted in different ways. Huang et al. (2008),
297 who studied the Dajiuhu peat deposit in China, used *des*-A-lupane as a proxy for the
298 depositional environment at the time of burial, linking sections of the biomarker record with
299 more *des*-A-lupane to episodes of limited degradation (i.e. better preservation). This
300 mechanism is less likely to apply to Lake Challa, because of its relatively constant
301 sedimentation rate and continuously anoxic bottom-water conditions. In a study on the
302 Brazilian Lake Caçó, *des*-A-lupane was thought to be derived from a belt of spike-rush
303 (*Eleocharis* sp.), an emergent aquatic macrophyte (Jacob et al., 2007). As already mentioned,
304 aquatic macrophytes are not a likely source of organic matter input in Lake Challa, as the
305 shoreline of Lake Challa is rocky and near-vertical (Fig. 1), which largely prevents aquatic
306 macrophyte growth. Even substantial lake-level lowering, which occurred during the early
307 late-glacial period (Moernaut et al. 2010), is not expected to have created more favorable
308 conditions for development of aquatic macrophytes (Sinninghe Damsté et al., 2011). Given
309 the absence of functionalized triterpenoids in the sedimentary record of Lake Challa, we
310 consider the sedimentary *des*-A-lupane record (Fig. 3) to reflect the input of its precursors in
311 the lake, with a constant transformation of these precursors into *des*-A-lupane, and minor or
312 no degradation of *des*-A-lupane over the last 25-kyr.

313 Most non-hopanoid triterpenoids are not species-specific, and the lupane-type
314 triterpenoids are no exception. Although these compounds occur in both C_3 and C_4 plants (e.g.
315 Misra et al., 1988; Macías-Rubalcava et al., 2007; Saleem, 2009; Singariya et al., 2012, 2014),
316 the specific $\delta^{13}C$ value of *des*-A-lupane (-27.4‰ on average, SD=±1.1‰, *n*=38; Fig. 4)
317 clearly indicates a C_3-plant origin (*cf.* Castañeda et al., 2009; Diefendorf et al., 2012).
318 Regnery et al. (2013) reported a comparable $\delta^{13}C$ signature (ranging from -28‰ to -30.6‰)
319 of *des*-A-lupane in lake sediments from the Holsteinian interglacial (*cf.* Marine Isotope Stage
320 11c) at Dethlingen in Germany, also similar to *des*-A-lupane isotope values in Tertiary brown
321 coal from China (-28.1±0.6‰; Schoell et al., 1994). Some genera of the Betulaceae (birch
322 family) biosynthesize *des*-A-lupane precursors and, therefore, this C_3 plant family is regularly
323 designated as an important biological source of *des*-A-lupane (Regnery et al., 2013; Schnell et
324 al., 2014). However, Betulaceae do not naturally occur in tropical Africa and no Betulaceae
325 vegetation or pollen are found in Lake Challa (van Geel et al., 2011; Sinninghe Damsté et al.,
326 2011), so in this setting, *des*-A-lupane must originate from other C_3-plant species.
327 In line with Regnery et al. (2013), and in contrast to Jacob et al. (2007), Huang et al.
328 (2008) and Diefendorf et al. (2012), the concentration of *des*-A-lupane in Lake Challa
329 sediments correlates well with oleanane- and ursane-type *des*-A-triterpenoids. We propose
330 that this dichotomy can be explained by one or more different sources of *des*-A-lupane in
331 these latter studies.
332 An interesting feature of the *des*-A-lupane $\delta^{13}C$ record is the apparent lack of trend
333 over longer timescales (Fig. 4). This record does show some variability over time, but,
334 unexpectedly, no trend, even though large changes in pCO_2 (and its carbon isotopic
335 composition), rainfall and vegetation occur over the glacial-interglacial transition. Recently it
336 was shown that carbon isotope discrimination in C_3 land plants is independent of natural
337 variations in *p*CO2 (e.g. Kohn, 2016). Furthermore, the $\delta^{13}C$ value of CO_2 varies by only

~1‰ (between -7‰ and -6‰) over the LGM and Holocene, a variability that is hard to differentiate within the analytical error margins of compound specific $\delta^{13}C$ analysis. Lastly, the modest variability in the *des*-A-lupane $\delta^{13}C$ record in Lake Challa that does occur shows no clear connection to the regional vegetation changes and the alternation of wetter and drier periods documented from other proxies. This absence of a clear trend in $\delta^{13}C$ values of *des*-A-lupane was also noted by Regnery et al. (2013) in their interglacial record from Dethlingen paleolake.

Recent studies have indicated the need for more direct proxies of C_3 and C_4 higher plants (Diefendorf et al., 2010; Castañeda and Schouten, 2011), and our findings may be an important step in this development. Firstly, the concentration of *des*-A-triterpenoids with ursane/oleanane/lupane skeletons in the Lake Challa record is high when C_3 plants (trees and shrubs) are common in local/regional vegetation (van Geel et al., 2011; Sinninghe Damsté et al., 2011). Therefore, we might be able to use these compounds as an absolute measure of C_3 plant abundance, instead of the usual estimate of C_3 or C_4 percentage based on variation in *n*-alkane $\delta^{13}C$ values. Secondly, we introduce a new way of estimating the average $\delta^{13}C$ value of C_3 vegetation at any point in time, which can be important for carbon cycle studies, as $\delta^{13}C$ records of C_3 plants could be used by modelers to assess the possible pCO_2-effect of plant $\delta^{13}C$ (Kohn, 2016). Thirdly, we can use this C_3-plant specific $\delta^{13}C$ record for improving estimates of the C_3/C_4 ratio in past vegetation. Recently, the relative contribution of C_3 and C_4 plants in terrestrial vegetation has been modeled using the $\delta^{13}C$ value of long-chain *n*-alkanes (e.g. Castañeda et al., 2007; Sinninghe Damsté et al., 2011; Berke et al., 2012). In the Holocene section of our Lake Challa record, *des*-A-lupane $\delta^{13}C$ values are on average less depleted (-27.6‰) than those off the *n*-C_{31} alkane (-29.1‰; Sinninghe Damsté et al., 2011); the situation is reversed during the glacial period, where average *des*-A-lupane $\delta^{13}C$ values (-27.2‰) are more depleted than those of *n*-C_{31} alkanes (-24.3‰; Sinninghe Damsté et al.,

2011). During the Holocene period, C_3 plants are estimated to contribute ca. 50% of the *n*-C_{31} alkanes (Sinninghe Damsté et al., 2011). This value was calculated using a simple binary box model, in which a 50/50 mixture of C_3- and C_4-derived alkanes (with mean values of respectively -35.2‰ and -21.7‰ in modern plants; Castañeda et al., 2009) yields an average $\delta^{13}C$ value of -28.5‰. During the glacial period, vegetation in the Lake Challa region was dominated by C_4 grasses; the mixed C_3/C_4 composition developed only from 16.5 kyr BP onwards (Sinninghe Damsté et al., 2011), when a riparian forest of C_3 trees and shrubs started growing inside the crater (van Geel et al., 2011). This local growth of C_3 vegetation is also clearly evident in the record of *des*-A-triterpenoid hydrocarbons with lupane, ursane and oleanane skeletons (Fig. 3).

The carbon isotopic fractionation between acetyl CoA-based compounds (e.g. *n*-alkanes) and the isoprene-based isoprenoids essentially depends on the biosynthetic pathways by which they are produced (e.g. MVA for isoprenoids in angiosperms). In their study of North American C_3 plants, Diefendorf et al. (2012) showed that this biosynthetic offset between terpenoids and n-alkanes is ~4-6‰. Correspondingly, also in sedimentary records, the ^{13}C of terpenoids is typically reported to be enriched by 5-6‰ compared to *n*-alkanes. We do not expect this biosynthetic offset between triterpenoids and *n*-alkanes to be different in East African vegetation. Temperate C_3 plants may have significantly lower 'overall' lipid fractionation values compared to tropical species (Diefendorf et al., 2011), but this will influence the *n*-alkanes and the terpenoids in the same way. Hence, we can use the $\delta^{13}C$ of *des*-A-lupane as a temporal (i.e. time-specific) C_3 endmember in modeling the C_3/C_4 ratio of local vegetation. To this end we subtracted an average terpenoid enrichment of 5.5‰ from the individual *des*-A-lupane $\delta^{13}C$ values of to estimate the $\delta^{13}C$ values of *n*-C_{31} alkanes derived from local C_3-plants at each time interval. We use the average offset as recorded in sediments (Diefendorf et al., 2012) for this down-core correction exercise, as sediments contain more

integrated, averaged signals compared to fresh plant material. Introduction of these corrected *n*-C_{31} alkane $\delta^{13}C$ values in the binary box model for C_3/C_4 ratio calculation, using a constant *n*-C_{31} alkane $\delta^{13}C$ value of -21.7‰ derived from C_4 plants (*cf.* Castañeda et al., 2009), results in an estimated increase inthe relative proportion of C_3 plants by 0 and 19% (Fig. 5) as compared to values obtained by Sinninghe Damsté et al. (2011). Our $\%C_3$ estimates are different from the previous estimates (t-test; $p<0.0001$, $n=35$), and the difference remains significant throughout the terpenoid to *n*-alkane offset range of 4 to 6‰ (i.e. the range that exists in modern plants; Diefendorf et al., 2012). From this exercise we conclude that especially in the Holocene part of the Lake Challa record, when local vegetation had a mixed C_3/C_4 composition, a reconstruction using fixed C_3-plant $\delta^{13}C$ values underestimates the fraction of C_3 vegetation, while there is less discrepancy during the glacial and early late-glacial periods when C_4 plants (here mostly grasses) were dominant. This result is especially valuable for carbon-cycle modeling studies, where correct assessment of climate-vegetation feedbacks strongly depends on correct estimates of past C_3/C_4 (and hence biome) distribution.

Our method for time-specific correction of the fraction of C_3 plants in local vegetation has the potential to enhance the accuracy of C_3/C_4 vegetation reconstructions in all situations where the local C_3-plant signal is as strong as during the Holocene around Lake Challa (Fig. 5). Using sample-specific *des*-A-triterpenoid $\delta^{13}C$ values for estimating this local C_3 vegetation component is convenient, as for example *des*-A-lupane is present in the saturated aliphatic lipid fraction, just like the *n*-alkanes, and can therefore be measured in the same analysis.

5. Conclusion

We investigated the possibility to use the degradation products of terrestrial higher plant pentacyclic triterpenoids as a proxy for local vegetation reconstructions. The accumulation of

413 *des*-A-triterpenoids with oleanane/ursane/lupane skeletons serves as a proxy record for the
414 local abundance of C_3 vegetation. The $\delta^{13}C$ signature of *des*-A-lupane can be used as a proxy
415 for the stable carbon isotopic composition of local C_3 plants if, as in our study site of Lake
416 Challa, *des*-A-lupane is exclusively of C_3-plant origin. Therefore, it can be applied as a
417 temporally variable C_3-plant end member representing the local C_3 vegetation component in
418 reconstructions of the C_3/C_4 ratio through time.
419

420 **Acknowledgements**

421 Sample collection for this study was carried out with permission of the Permanent Secretary
422 of the Ministry of Education, Science and Technology of Kenya under research permit
423 13/001/11C to D.V. This work was performed as contribution to the ESF EuroClimate project
424 CHALLACEA and the ICDP project DeepCHALLA, financially supported mainly by grants
425 from the Dutch Organization for Scientific Research (NWO) and FWO-Vlaanderen (Belgium)
426 to J.S.S.D. and D.V., respectively. Part of the work was carried out under the program of the
427 Netherlands Earth System Science Centre (NESSC), financially supported by the Ministry of
428 Education, Culture and Science (OCW). We thank C.M. Oluseno for field assistance, and A.
429 Mets, M. Verweij, J. Ossebaar and M. van der Meer for technical assistance. We further thank
430 J. Jacob and an anonymous reviewer for their valuable comments, which greatly improved
431 this manuscript.
432

433 **References**

434 Baas, W.J., 1985. Naturally occurring *seco*-ring-A-triterpenoids and their possible biological
435 significance. Phytochemistry 24, 1875-1889.
436 Berke, M.A., Johnson, T.C., Werne, J.P., Grice, K., Schouten, S., Sinninghe Damsté, J.S.,
437 2012. Molecular records of climate variability and vegetation response since the Late

438 Pleistocene in the Lake Victoria basin, East Africa. Quaternary Science Reviews 55,
439 59-74.
440 Blaauw, M., van Geel, B., Kristen, I., Plessen, B., Lyaruu, A., Engstrom, D.R., van der Plicht,
441 J., Verschuren, D., 2011. High-resolution ^{14}C dating of a 25,000-year lake-sediment
442 record from equatorial East Africa. Quaternary Science Reviews 30, 3043-3059.
443 Boreham, C.J., Summons, R.E., Roksandic, Z., Dowling, L.M., Hutton, A.C., 1994.
444 Chemical, molecular and isotopic differentiation of organic facies in the Tertiary
445 lacustrine Duaringa oil shale deposit, Queensland, Australia. Organic Geochemistry
446 21, 685-712.
447 Bossard, N., Jacob, J., Le Milbeau, C., Sauze, J., Terwilliger, V., Poissonnier, B., Vergès, E.,
448 2013. Distribution of miliacin (olean-18-en-3β-ol methyl ether) and related
449 compounds in broomcorn millet (*Panicum miliaceum*) and other reputed sources:
450 Implications for the use of sedimentary miliacin as a tracer of millet. Organic
451 geochemistry 63, 48-55.
452 van Bree, L.G.J., Rijpstra, W.I.C., Cocquyt, C., Al-Dhabi, N.A., Verschuren, D., Sinninghe
453 Damsté, J.S., de Leeuw, J.W., 2014. Origin and palaeo-environmental significance of
454 C_{25} and C_{27} *n*-alk-1-enes in a 25,000-year lake-sedimentary record from equatorial
455 East Africa. Geochimica et Cosmochimica Acta 145, 89-102.
456 Buckles, L.K., Weijers, J.W.H., Verschuren, D., Sinninghe Damsté, J.S., 2014. Sources of
457 core and intact branched tetraether membrane lipids in the lacustrine environment:
458 Anatomy of Lake Challa and its catchment, equatorial East Africa. Geochimica et
459 Cosmochimica Acta 140, 106-126.
460 Castañeda, I.S., Werne, J.P., Johnson, T.C., 2007. Wet and arid phases in the southeast
461 African tropics since the Last Glacial Maximum. Geology 35, 823–826.

462 Castañeda, I.S., Mulitza, S., Schefuß, E., Lopes dos Santos, R.A., Sinninghe Damsté, J.S.,
463 Schouten, S., 2009. Wet phases in the Sahara/Sahel region and human migration
464 patterns in North Africa. Proceedings of the National Academy of Sciences of the
465 United States of America 106, 20159–20163.
466 Castañeda, I.S., Schouten, S., 2011. A review of molecular organic proxies for examining
467 modern and ancient lacustrine environments. Quaternary Science Reviews 30, 2851-
468 2891.
469 Corbet, B., 1980. Origine et transformation des triterpènes dans les sédiments récents. Ph.D.
470 thesis, Université Louis Pasteur, Strasbourg, France, 106 p.
471 Diefendorf, A.F., Mueller, K.E., Wing, S.L., Koch, P.L., Freeman, K.H., 2010. Global
472 patterns in leaf ^{13}C discrimination and implications for studies of past and future
473 climate. Proceedings of the National Academy of Sciences of the United States of
474 America 103, 5738-5743.
475 Diefendorf, A.F., Freeman, K.H., Wing, S.L., Graham., H.V., 2011. Production of *n*-alkyl
476 lipids in living plants and implications for the geological past. Geochimica et
477 Cosmochimica Acta 75, 7472-7485.
478 Diefendorf, A.F., Freeman, K.H., Wing, S.L., 2012. Distribution and carbon isotope patterns
479 of diterpenoids and triterpenoids in modern temperate C_3 trees and their geochemical
480 significance. Geochimica et Cosmochimica Acta 85, 342-356.
481 Freeman, K.H., Boreham, C.J., Summons, R.E., Hayes, J.M., 1994. The effect of
482 aromatization on the isotopic compositions of hydrocarbons during early diagenesis.
483 Organic Geochemistry 21, 1037–1049.
484 van Geel, B., Gelorini, V., Lyaruu, A., Aptroot, A., Rucina, S., Marchant, R., Sinninghe
485 Damsté, J.S., Verschuren, D., 2011. Diversity and ecology of tropical African fungal

spores from a 25,000-year palaeoenvironmental record in southeastern Kenya. Review of Palaeobotany and Palynology 164, 174-190.

Hauke, V., Graff, R., Wehrung, P., Trendel, J.M., Albrecht, P., 1992a. Novel triterpene-derived hydrocarbons of arborane/fernane series in sediments. Part I. Tetrahedron 48, 3915-3924.

Hauke, V., Graff, R., Wehrung, P., Trendel, J.M., Albrecht, P., Riva, A., Hopfgartner, G., Gülaçar, F.O., Buchs, A., Eakin, P.A., 1992b. Novel triterpene-derived hydrocarbons of arborane/fernane series in sediments. Part II. Geochimica et Cosmochimica Acta 56, 3595-3602.

ten Haven, H.L., Rullkötter, J., 1988. The diagenetic fate of taraxer-14-ene and oleanene isomers. Geochimica et Cosmochimica Acta 10, 2543-2548.

Hemp, A., 2006. Continuum or zonation? Altitudinal gradients in the forest vegetation of Mt. Kilimanjaro. Plant Ecology 184, 27-42.

Huang, X., Xie, S., Zhang, C.L., Jiao, D., Huang, J., Yu, J., Jin, F., Gu, Y., 2008. Distribution of aliphatic *des*-A-triterpenoids in the Dajiuhu peat deposit, southern China. Organic Geochemistry 39, 1765-1771.

Jacob, J., Disnar, J.R., Boussafir, M., Albuquerque, A.L.S., Sifeddine, A., Turcq, B., 2007. Contrasted distributions of triterpene derivatives in the sediments of Lake Caçó reflect paleoenvironmental changes during the last 20,000 yrs in NE Brazil. Organic Geochemistry 38, 180-197.

Kohn, M.J., 2016. Carbon isotope discrimination in C_3 land plants is independent of natural variations in pCO_2. Geochemical Perspective Letters 2, 35-43.

Langenheim, J.H., 1994. Higher plant terpenoids: A phytocentric overview of their ecological roles. Journal of Chemical Ecology 20, 1223-1280.

510 Logan, G.A., Eglinton, G., 1994. Biogeochemistry of the Miocene lacustrine deposit, at
511 Clarkia, northern Idaho, U.S.A. Organic Geochemistry 21, 857-870.
512 Lohmann, F., Trendel, J.M., Hetru, C., Albrecht, P., 1990. C-29 tritiated β-amyrin: chemical
513 synthesis aiming at the study of aromatization processes in sediments. Journal of
514 Labelled Compounds and Radiopharmaceuticals 28, 377-386.
515 Macías-Rubalcava, M.L., Hernández-Bautista, B.E., Jiménez-Estrada, M., Cruz-Ortega, R.,
516 Anaya, A.L., 2007. Pentacyclic triterpenes with selective bioactivity from Sebastiania
517 adenophora leaves, Euphorbiaceae. Journal of Chemical Ecology 33, 147-156.
518 Misra, S., Choudhury, A., Chattopadhyay, S., Ghosh, A., 1988. Lipid composition of
519 Porteresia coarctata from two different mangrove habitats in India. Phytochemistry 27,
520 361-364.
521 Moernaut, J., Verschuren, D., Charlet, F., Kristen, I., Fagot, M., De Batist, M., 2010. The
522 seismic-stratigraphic record of lake-level fluctuations in Lake Challa: Hydrological
523 stability and change in equatorial East Africa over the last 140 kyr. Earth and
524 Planetary Science Letters 290, 214-223.
525 Ohmoto, T., Ikuse, M., Natori, S., 1970. Triterpenoids of the Gramineae. Phytochemistry 9,
526 2137-2148.
527 Regnery, J., Püttmann, W., Koutsodendris, A., Mulch, A., Pross, J., 2013. Comparison of the
528 paleoclimatic significance of higher land plant biomarker concentrations and pollen
529 data: A case study of lake sediments from the Holsteinian interglacial. Organic
530 Geochemistry 61, 73-84.
531 Rullkötter, J., Leythaeuser, D., Wendisch, D., 1982. Novel 23,28-bisnorlupanes in Tertiary
532 sediments. Widespread occurrence of nuclear demethylated triterpanes. Geochimica et
533 Cosmochimica Acta 46, 2501-2509.

534 Sabel, M., Bechtel, A., Püttmann, W., Hoernes, S., 2005. Palaeoenvironment of the Eocene
535 Eckfeld Maar lake (Germany): implications from geochemical analysis of the oil shale
536 sequence. Organic Geochemistry 36, 873-891.
537 Saleem, M., 2009. Lupeol. A novel anti-inflammatory and anti-cancer dietary triterpene.
538 Cancer Letters 285, 109-115.
539 Schmitter, J.M., Arpino, P.J., Guiochon, G., 1981. Isolation of degraded pentacyclic
540 triterpenoid acids in a Nigerian crude oil and their identification as tetracyclic
541 carboxylic acids resulting from ring A cleavage. Geochimica et Cosmochimica Acta
542 45, 1951-1955.
543 Schnell, G., Schaeffer, P., Tardivon, H., Motsch, E., Connan, J., Ertlen, D., Schwartz, D.,
544 Schneider, N., Adam, P., 2014. Contrasting diagenetic pathways of higher plant
545 triterpenoids in buried wood as a function of tree species. Organic Geochemistry 66,
546 107-124.
547 Schoell, M., Simoneit, B.R.T., Wang, T.G., 1994. Organic geochemistry and coal petrology of
548 Tertiary brown coal in the Zhoujing mine, Baise Basin, South China – 4. Biomarker
549 sources inferred from stable carbon isotope compositions of individual compounds.
550 Organic Geochemistry 21, 713–719.
551 Singariya, P., Kumar, P., Mourya, K.K., 2012. Isolation of some new steroids and evaluation
552 of bio-activity of Cenchrus ciliaris. International Journal of Research in
553 Pharmaceutical Sciences 3, 678-684.
554 Singariya, P., Kumar, P., Mourya, K.K., 2014. Isolation of new steroids of Kala Dhaman
555 grass (Cenchrus setigerus) and evaluation of their bioactivity. Brazilian Archives of
556 Biology and Technology 57, 62-69.
557 Sinninghe Damsté, J.S., Ossebaar, J., Abbas, B., Schouten, S., Verschuren, D., 2009. Fluxes
558 and distribution of tetraether lipids in an equatorial African lake: Constraints on the

559 application of the TEX_{86} palaeothermometer and BIT index in lacustrine settings.
560 Geochimica et Cosmochimica Acta 73, 4232-4249.
561 Sinninghe Damsté, J.S., Verschuren, D., Ossebaar, J., Blokker, J., van Houten, R., van der
562 Meer, M.T.J., Plessen, B., Schouten, S., 2011. A 25,000-year record of climate-
563 induced changes in lowland vegetation of eastern equatorial Africa revealed by the
564 stable carbon-isotopic composition of fossil plant leaf waxes. Earth and Planetary
565 Science Letters 302, 236-246.
566 Sinninghe Damsté, J.S., Ossebaar, J., Schouten, S., Verschuren, D., 2012. Distribution of
567 tetraether lipids in the 25-ka sedimentary record of Lake Challa: extracting reliable
568 TEX_{86} and MBT/CBT palaeotemperatures from an equatorial African lake. Quaternary
569 Science Reviews 50, 43-54.
570 Smetanina, O.F., Kuznetzova, T.A., Denisenko, V.A., Pivkin, M.V., Khudyakova, Y.V.,
571 Gerasimenko, A.V., Popov, D.Y., Il'in, S.G., Elyakov, G.B., 2001. 3β-methoxyolean-
572 18-ene (miliacin) from the marine fungus *Chaetomium olivaceum*. Russian Chemical
573 Bulletin 50, 2463-2465.
574 Trendel, J.M., Lohmann, F., Kintzinger, J.P., Albrecht, P., Chiarone, A., Riche, C., Cesario,
575 M., Guilhem, J., Pascard, C., 1989. Identification of *des*-A-triterpenoid hydrocarbons
576 occurring in surface sediments. Tetrahedron 6, 4457-4470.
577 Verschuren, D., Sinninghe Damsté, J.S., Moernaut, J., Kristen, I., Blaauw, M., Fagot, M.,
578 Haug, G.H., 2009. Half-precessional dynamics of monsoon rainfall near the East
579 African Equator. Nature 462, 637-641.
580 Wolff, C., Haug, G.H., Timmermann, A., Sinninghe Damsté, J.S., Brauer, A., Sigman, D.M.,
581 Cane, M.A., Verschuren, D., 2011. Reduced interannual rainfall variability in East
582 Africa during the Last Ice Age. Science 333, 743-747.
583 Wolff, C., Kristen-Jenny, I., Schettler, G., Plessen, B., Meyer, H., Dulski, P., Naumann, R.,
584 Brauer, A., Verschuren, D., Haug, G.H., 2014. Modern seasonality in Lake Challa

(Kenya/Tanzania) and its sedimentary documentation in recent lake sediments. Limnology and Oceanography 59, 1621-1636.

Figure legends

Figure 1: [A] Location of Lake Challa (3°19'S, 37°42'E) in equatorial East Africa. [B] Lake Challa and its crater basin with bathymetry at 10-m intervals and sampling locations of the suspended particulate matter (SPM) profile (▲), the sediment trap (□) and the 25,000-year sediment record (■), as well as catchment soils (○) and litter (●). The outer bold line indicates the crater rim, which defines the lake's catchment area. Modified after Moernaut et al. (2010) and van Bree et al. (2014).

Figure 2: Higher plant derived *des*-A-triterpenoids in the Lake Challa sediments. Panel [A] shows a partial summed mass chromatogram (*m/z* 163+177+189+203+218+309) of the distribution of *des*-A-triterpenoids in the apolar fraction of the lipid biomarker extract from 996-1000 cm core depth, deposited ~12.1 kyr BP. Panel [B] shows the electron-impact mass spectra of *des*-A-triterpenoids in the Lake Challa sediment record: *des*-A-olean-13(18)-ene (compound **1**); *des*-A-olean-12-ene (**2**); *des*-A-urs-13(18)-ene (**3**); mixture of *des*-A-ursenes (**4**); *des*-A-lupane (**5**). Additional information on these compounds is presented in Table 1.

Figure 3: Variation through time in the accumulation rates (in mg m^{-2} yr^{-1}, not cumulative) of the *des*-A-triterpenoid compounds for *des*-A-lupane, *des*-A-ursenes and *des*-A-oleanenes in Lake Challa sediments. Shaded areas represent the LGM (26.5-19 kyr BP), Heinrich event H1 (16.8-15.4 kyr BP) and YD (13-11.5 kyr BP).

609 Figure 4: Variation through time in the stable carbon isotopic composition ($\delta^{13}C$, in ‰ vs.
610 VPDB) of *n*-C_{31} alkanes (Sinninge Damsté et al., 2011) and *des*-A-lupane (this study).
611
612 Figure 5: Percentage of C_3 vegetation, based on *n*-C_{31} alkane $\delta^{13}C$ values (data from
613 Sinninghe Damsté et al., 2011), calculated in two different ways: first (solid line) using *des*-
614 A-lupane as the local and temporally variable C_3-plant endmember and an average terpenoid
615 fractionation of 5.5‰ relative to the *n*-alkanes,and second (dashed line) based on fixed $\delta^{13}C$
616 values for the C_3-plant (-35.2‰) and C_4-plant (-21.7‰) endmembers taken from the literature
617 (Sinninghe Damsté et al., 2011). The range of C_3 estimates when the modern terpenoid
618 fractionation range of 4 to 6‰ is taken into account is plotted as a grey band. Boxplots show
619 the differences between the original and *des*-A-lupane (grey, left-hand side) corrected C_3
620 estimate in the glacial and early late-glacial (25 to 16 kyr BP) and in the interglacial period
621 (Holocene, 12.3 to 0 kyr BP) (thus excluding the glacial-interglacial transition), with median,
622 first and third quartiles, and whiskers depicting the minimum/maximum values.
623
624 Table 1: List of *des*-A-triterpenoids in the Lake Challa sediment record with retention times,
625 mass spectral data and (tentative) identifications. References: **A**: Corbet (1980); **B**: Logan and
626 Eglinton (1994); **C**: Trendel et al. (1989); **D:** Jacob et al. (2007); **E**: Huang et al. (2008); **F:**
627 Schmitter et al. (1981); **G:** Boreham et al. (1994)

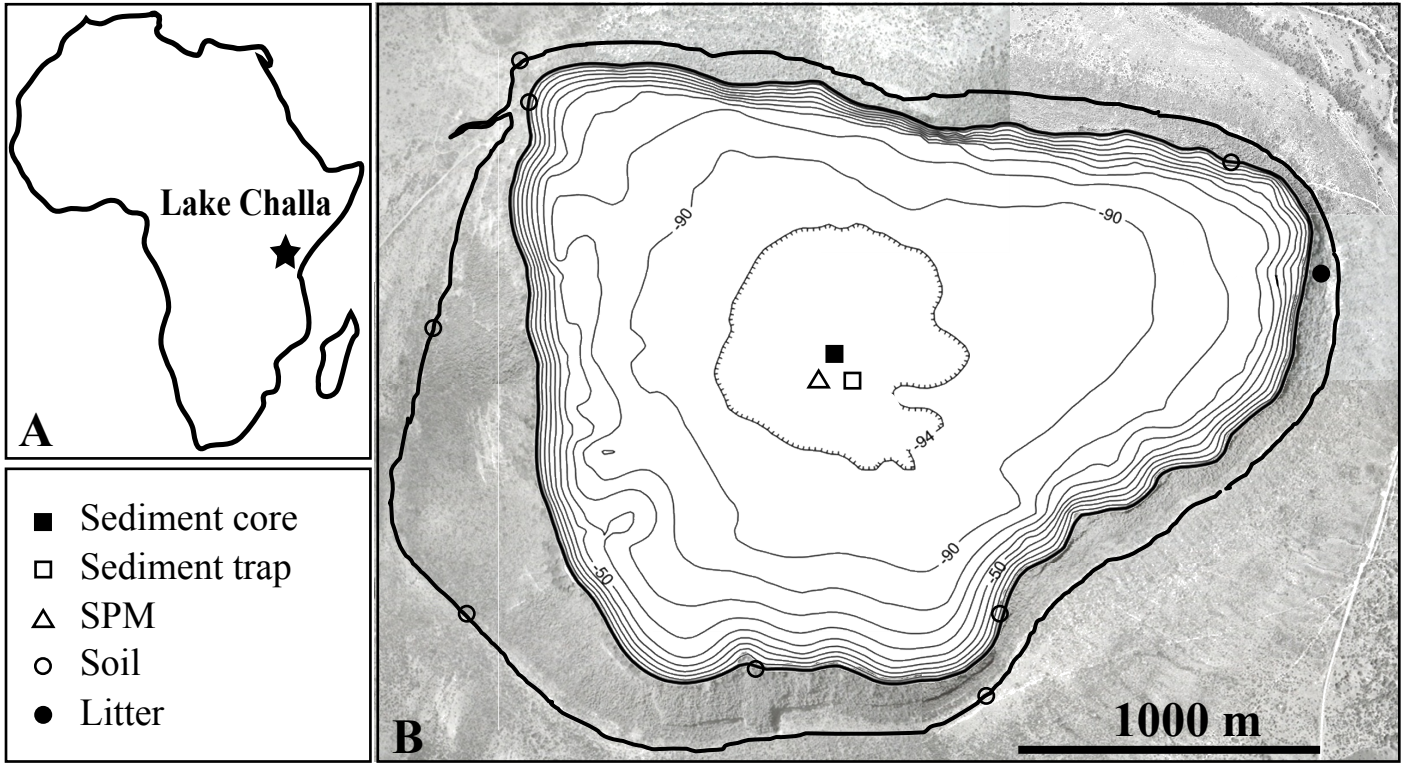
Lake Challa
A
Sediment core
Sediment trap
SPM
Soil
Litter
-90
-90
-94
-90
-50
-50
B
1000 m

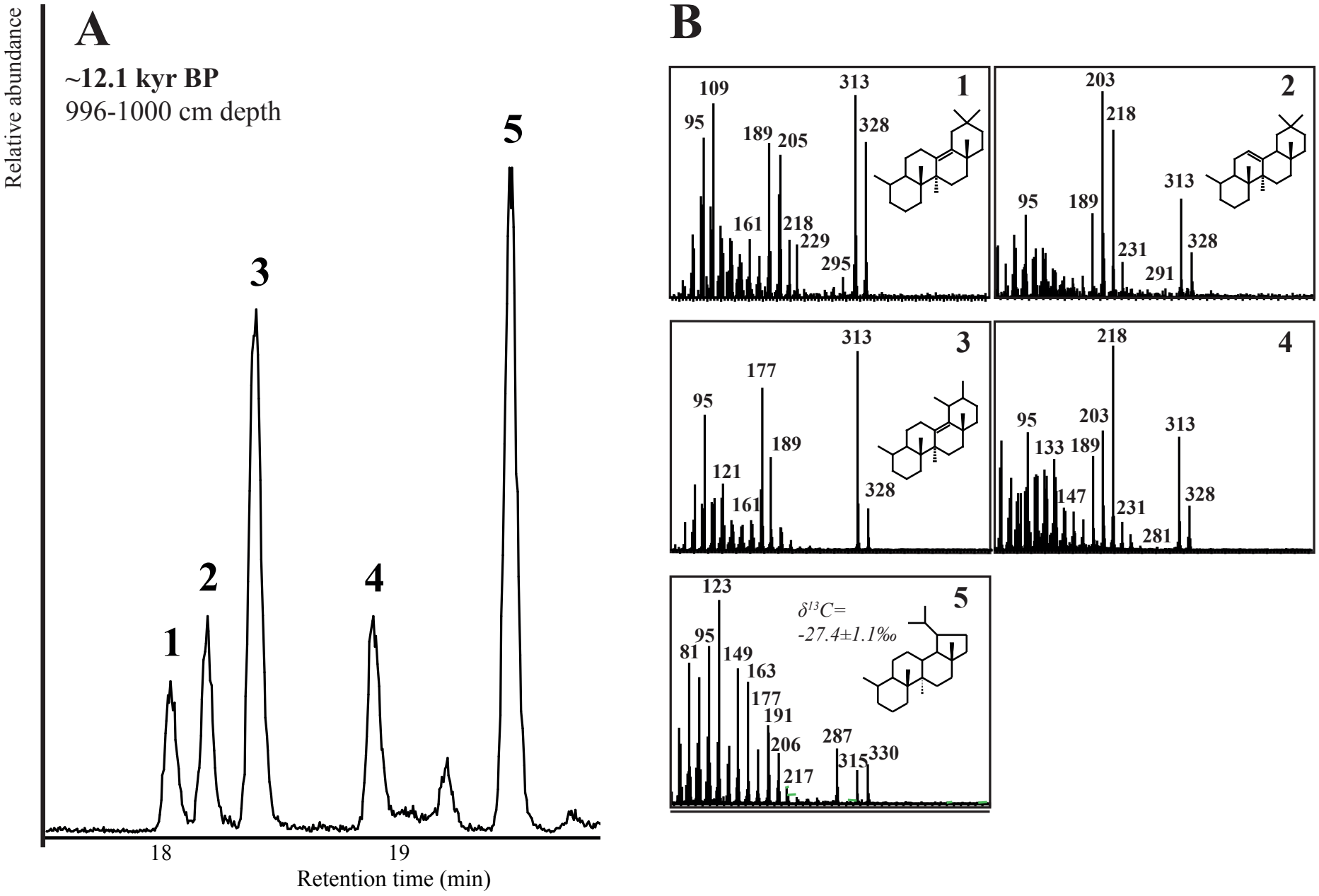
A
~12.1 kyr BP
996-1000 cm depth
Relative abundance
1
2
3
4
5
18
19
Retention time (min)
B
1
109
95
189
205
313
328
161
218
229
295
2
203
218
95
189
313
231
328
291
3
313
177
95
189
121
161
328
4
218
95
203
313
133
189
147
231
328
281
5
123
95
81
149
163
177
191
206
217
287
315
330
δ13C=
-27.4±1.1‰

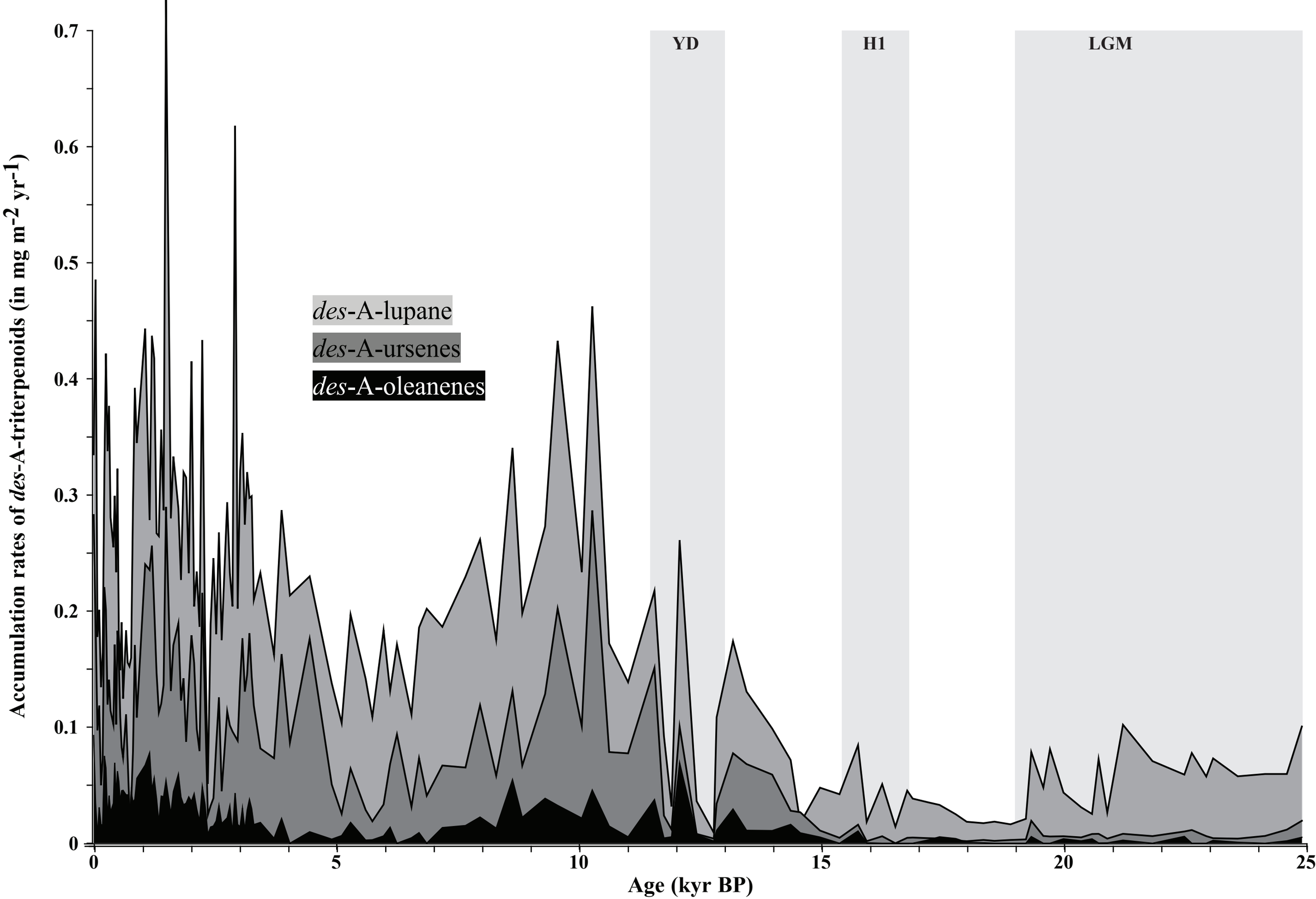
YD
H1
LGM
des-A-lupane
des-A-ursenes
des-A-oleanenes
Accumulation rates of des-A-triterpenoids (in mg m-2 yr-1)
0
0.1
0.2
0.3
0.4
0.5
0.6
0.7
0
5
10
15
20
25
Age (kyr BP)

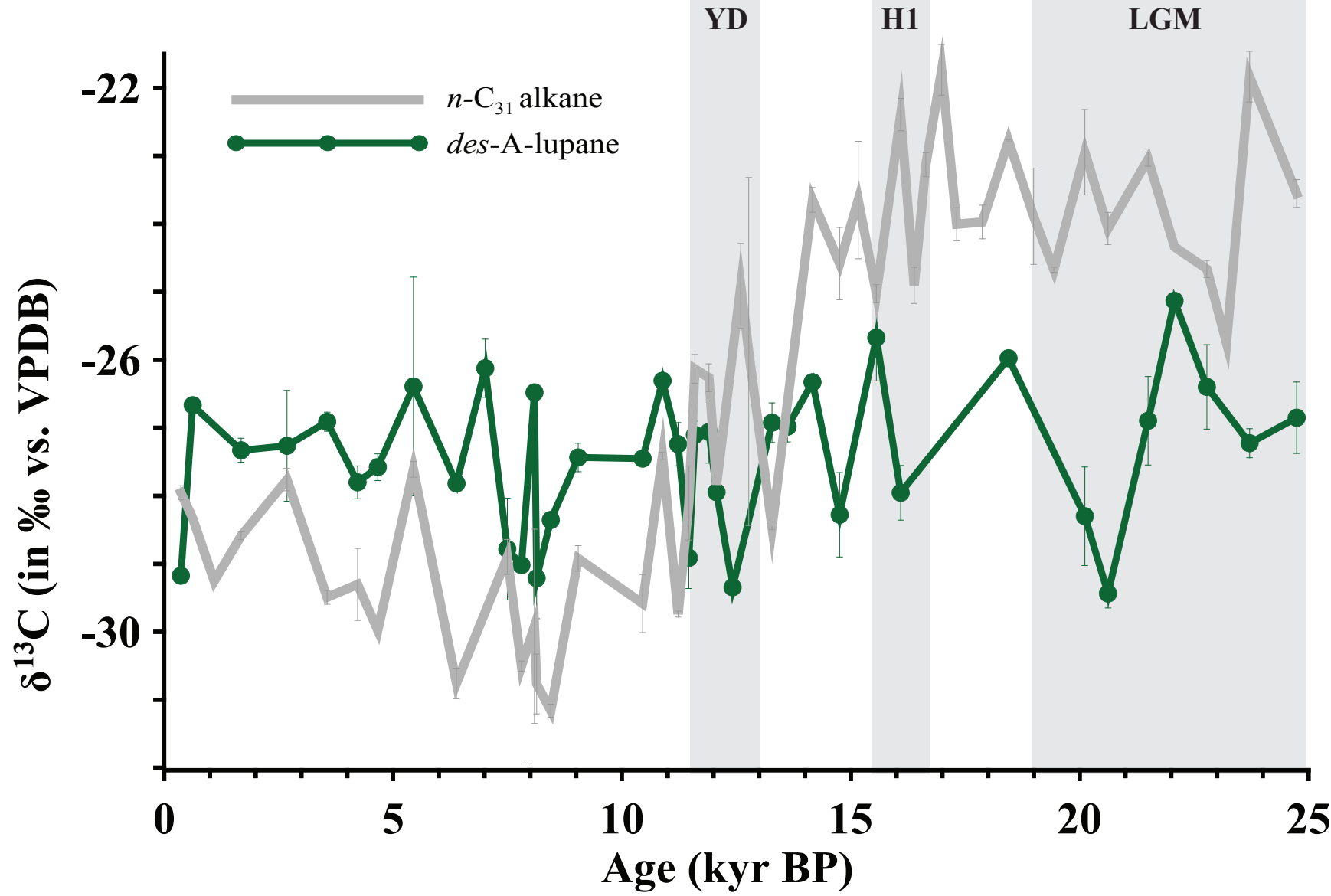
YD
H1
LGM
-22
-26
-30
n-C31 alkane
des-A-lupane
δ13C (in ‰ vs. VPDB)
0
5
10
15
20
25
Age (kyr BP)

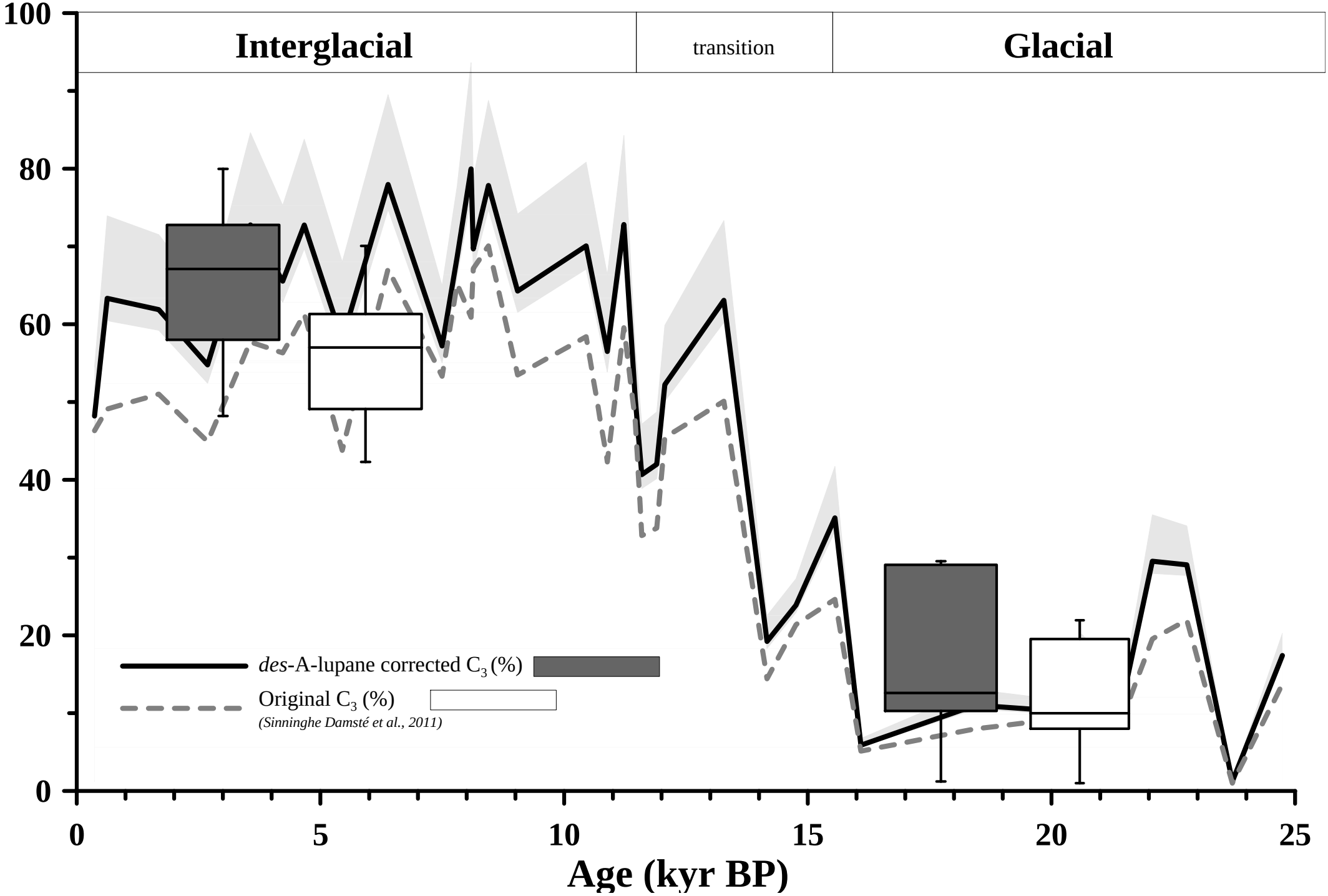
Interglacial
transition
Glacial
100
80
60
40
20
0
0
5
10
15
20
25
Age (kyr BP)
des-A-lupane corrected C3 (%)
Original C3 (%)
(Sinninghe Damsté et al., 2011)

Peak number	Retention time (GCMS)	Most significant ions (in order of decreasing abundance)	M^+	Formula	Tentative identification	References
1	18.16	109, 313, 189, 328 [M^+], 205, 204, 218, 161	328	$C_{24}H_{40}$	*Des*-A-olean-13(18)ene	A B C D E
2	18.30	203, 218, 313, 189, 328 [M^+], 231, 243	328	$C_{24}H_{40}$	*Des*-A-olean-12-ene	A B D
3	18.52	313, 177, 189, 121, 175, 328 [M^+], 218	328	$C_{24}H_{40}$	*Des*-A-urs-13(18)ene	A B D
4	19.01	218, 203, 313, 189, 133, 328 [M^+], 231	328	($C_{24}H_{40}$)	Mixture, *i.a. des*-A-ursenes	
5	19.60	123, 149, 163, 191, 287, 206, 330 [M^+], 315	330	$C_{24}H_{42}$	*Des*-A-lupane	A C D E F G